

PAPER • OPEN ACCESS

Structural and luminescent characteristics of YAG phosphors synthesized in the radiation field

To cite this article: D A Mussakhanov *et al* 2019 *IOP Conf. Ser.: Mater. Sci. Eng.* **510** 012031

View the [article online](#) for updates and enhancements.

You may also like

- [Effect of temperature and moisture on the luminescence properties of silicone filled with YAG phosphor](#)
Qin Zhang, , Feng Jiao et al.
- [Review—White Light-Emitting Diodes: Past, Present, and Future](#)
Noor Ul Islam, Muhammad Usman, Saad Rasheed et al.
- [Blue laser diode-pumped Ce:YAG phosphor-coated cylindrical rod-based extended white light source with uniform illumination](#)
Atul Kumar Dubey, Mayank Gupta, Virendra Kumar et al.



ECS The Electrochemical Society
Advancing solid state & electrochemical science & technology

242nd ECS Meeting

Oct 9 – 13, 2022 • Atlanta, GA, US

Early hotel & registration pricing ends September 12

Presenting more than 2,400 technical abstracts in 50 symposia

The meeting for industry & researchers in
BATTERIES
ENERGY TECHNOLOGY
SENSORS AND MORE!

 Register now!

 **ECS Plenary Lecture featuring M. Stanley Whittingham,**
Binghamton University
Nobel Laureate –
2019 Nobel Prize in Chemistry



Structural and luminescent characteristics of YAG phosphors synthesized in the radiation field

D A Mussakhanov¹, A T Tulegenova², V M Lisitsyn¹, M G Golkovsky³, L A Lisitsyna⁴, Kh A Abdullin², M B Aitzhanov², Zh Karipbayev⁵, A Kozlovsky⁵ and Yu I. Michailov⁶

¹National Research Tomsk Polytechnic University, Tomsk, 634050, Russia

²al-Farabi Kazakh National University, Almaty, 050040, Kazakhstan

³Institute of Nuclear Physics of Siberian Branch Russian Academy of Sciences, Novosibirsk, 630090, Russia

⁴Tomsk State University of Architecture and Building, Tomsk, 634003, Russia

⁵L.N. Gumilyov Eurasian National University, Astana, 010008, Kazakhstan

⁶Institute of Solid State Chemistry and Mechanochemistry, Siberian Branch of the Russian Academy of Sciences, Novosibirsk, 630128, Russia

E-mail: tulegenova.aida@gmail.com

Abstract. YAG:Ce, YAGG:Ce ceramics were obtained by sintering the oxide powders in the radiation field. The results of investigations of the structure, composition and luminescence of ceramics are presented. The luminescence characteristics of powders exactly correspond to the phosphors luminescence used in practice obtained by solid-state synthesis methods. It has been established that in the used radiation exposure modes the main factor determining the efficiency of the synthesis is the ionization density.

1. Introduction

YAG:Ce phosphors are the most promising for use in light-emitting diodes (LEDs). The phosphors are crystalline multicomponent systems. Their synthesis is usually carried out using solid-phase reactions [1–5].

The melting points of the components are high. Therefore, the reproducibility of the results of the synthesis is low: the elemental composition of microcrystals differs significantly from that in the mixture. The elemental composition of the phosphor of different batches changes even during synthesis under the same conditions and the same initial composition of the mixture. Fluorescent properties are also changing. This is explained by the strong influence on the result of the synthesis of uncontrolled deviations of technological modes in the synthesis process. Therefore, we are constantly working to improve the technology of phosphor preparation, the develop of new technologies. A particular difficulty in the preparation of the phosphor is the first stage - the production of ceramics by sintering the initial oxide powders.

This paper presents the results of studies of the structural and luminescent characteristics of phosphors synthesized using a fundamentally new method - sintering in the radiation field



2. Samples preparation

The charge was composed of a mixture of the following powders: Y_2O_3 (22 – 36 weight %), Al_2O_3 (56– 62 weight %), Ce_2O_3 (2.4 – 9.1 weight %) and Gd_2O_3 (0 – 12 weight %). The resulting mixture was poured into cavities with a depth of 5 mm of the massive copper crucible. A powerful electron flow directed from the vacuum to the medium with atmospheric pressure through a differential vacuum pumping system consisting of three stages was sent to the crucible. The electrons flow with the energy of 1.4 MeV and a power density of 22–25 KW per cm^2 from the ELV-6 accelerator was scanned along the crucible at a speed of 1 cm s^{-1} . The electron beam with a cross section at the surface of the crucible 1 cm^2 melted the charge for 1 s, which, after exposure, quickly hardened, forming a ceramic sample with a ratio of oxide components set by the charge composition. After cooling, the samples were removed from the crucible.

Figure 1 shows photographs of samples of synthesized YAG:Ce ceramics having a volume in the range of 0.8 to 1 cm^3 . Samples YAG:Ce had a yellow color. The samples containing gadolinium, as a modifier (YAGG: Ce), had dark yellow color. Excitation with a radiation chip with $\lambda = 460 \text{ nm}$ leads to luminescence of YAG: Ce in the green, YAGG: Ce - in the yellow region of the spectrum.



Figure 1. Photographs of samples of synthesized YAG: Ce ceramics illuminated by white light (the first picture) and excited by LED radiation (next two pictures)

From the pictures shown in the figure 1, it is clear that the luminescence is distributed non-uniformly over the sample surface. This is due to the inhomogeneous distribution of cerium oxide by volume of the charge and, accordingly, the dopant in terms of the volume of ceramics.

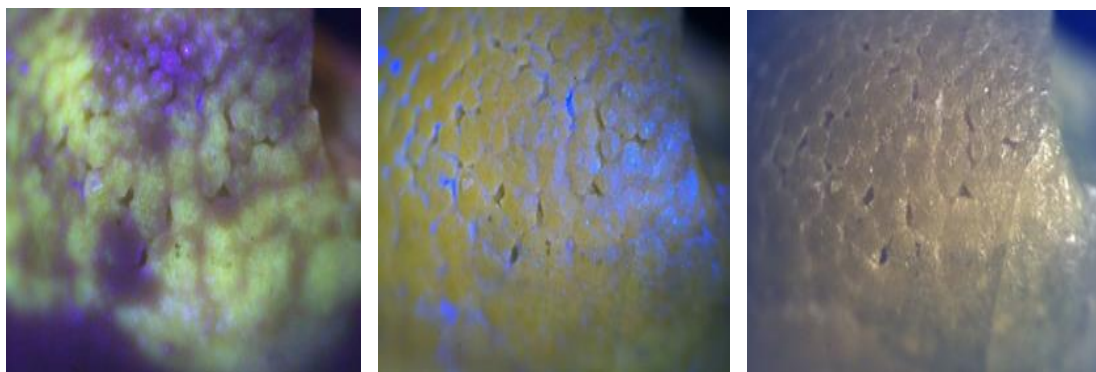


Figure 2. Photographs of one and the same surface area of a ceramic sample illuminated by light with $\lambda = 365$ and 450 nm from chips and an incandescent lamp (from left to right, respectively)

Figure 2 shows photographs of the one and the same surface area of ceramic sample illuminated by light from LED with $\lambda = 365$ and 450 nm and an incandescent lamp, respectively. The area of a picture

is $3 \times 2.5 \text{ mm}^2$. The synthesized sample of ceramics represents sticky fragments of a rounded shape. The fragments have a size of 100 - 200 microns. The fragments are firmly connected to each other. The photograph in white light shows that the crack passes along a plane unrelated to the shape of the fragment. Excitation by radiation from chips with $\lambda = 365$ and 450 nm leads to the appearance of luminescence. The fields of the luminescent regions differ in shape and color. When excited by radiation from a chip with $\lambda = 365$ nm, luminescence areas of yellow and purple are clearly distinguished, while excitation by radiation with $\lambda = 450$ nm leads only to yellow luminescence almost uniformly distributed over the samples surface. The difference is probably due to the fact that irradiation with $\lambda = 365$ nm excites, besides yellow, violet luminescence. The luminescence centers responsible for effective violet luminescence are unevenly distributed over the surface.

The surface state of the synthesized ceramics samples were studied using the Hitachi TM-3030 scanning electron microscope (SEM). The device made it possible to observe bulk samples with a shadow and volume contrast with a resolution of up to 30 nm. Figure 3 shows typical SEM images of the sample surface with an area of $\sim 0.016 \text{ mm}^2$, magnified 1000 times. There are snapshots of the surface of a ceramics samples prepared from charges with different composition: of Al_2O_3 (56.8 %) + Y_2O_3 (34.1 %) + Ce_2O_3 (9.1 %) (3a) and Al_2O_3 (59.5 %) + Y_2O_3 (23.8 %) + Gd_2O_3 (11.9 %) + Ce_2O_3 (4.8 %) (3b).

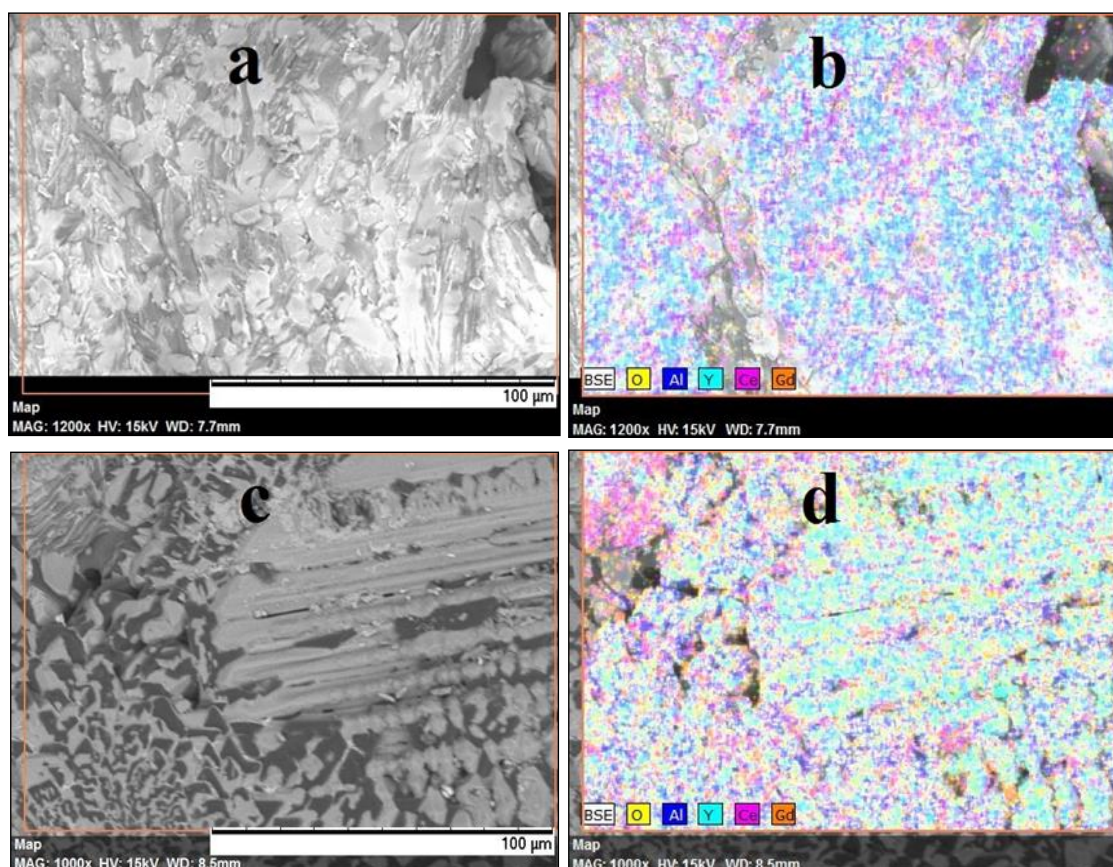


Figure 3. SEM images of samples surface with the different composition: (a) - Al_2O_3 (56.8 %) + Y_2O_3 (34.1%) + Ce_2O_3 (9.1 %); (c) - Al_2O_3 (59.5 %) + Y_2O_3 (23.8 %) + Gd_2O_3 (11.9 %) + Ce_2O_3 (4.8 %). Pictures b and d show the elemental composition distribution over the surface in these samples respectively

From presented images it is clear that the samples consist of glued particles, often of regular shapes. This suggests that crystal structure is formed under exposure to a radiation flow during the ceramics samples preparation.

3. Structure of synthesized YAG ceramics

The electron microscope with the Bruker XFlash MIN SVE has been chosen for the synthesized samples analysis. The elemental composition was determined in fragments of split samples of ceramics. The results of measurements are shown in Table 1. Samples 1 and 2 had the same initial composition of the charge. In table 1 different fragments of the same split sample of ceramics were represented. Ceramics sample 3 was prepared from the charge doped with Gd. The table 1 shows the elemental composition of different fragments of a crushed ceramic sample. The result presented in the table 1 show that the elemental composition in ceramic samples 1 and 2 is different, although the initial charge compositions, were the same. Compositional studies were conducted at different points on the plane of the fractured ceramic sample. There is a difference in the elemental composition over the surface. Consequently, during the synthesis of ceramics, a change in the elemental composition by volume occurs. There is a difference in the composition of the ceramic sample 3 from original composition of the charge.

Table 1. The elemental composition of the charge and ceramics samples prepared from it

Sample		Elemental composition, in %				
		O	Al	Y	Ce	Gd
1	In furnace-charge	60	25	11.9	3.1	-
	In ceramics	57.4	33.3	7.55	1.8	-
2	In furnace-charge	60	25	11.9	3.1	-
	In ceramics	66.3	25.6	7.49	0.54	-
3	In furnace-charge	60	25	7.92	3.18	3.9
	In ceramics	52.8	37.7	7.29	1.35	0.8

Obviously, the heterogeneity of physical and chemical processes during of the synthesis takes place. It means that the charge could not be mixed.

Nevertheless, there is a correspondence between the composition of the elements in the charge and ceramics samples. Figures 3b and 3d show the measured distribution of the elemental composition on arbitrarily selected areas of the cleavage sample surface. As it can be seen from the presented images, the elements of the composition are distributed relatively homogeneously. This indicates that in the synthesis process in the radiation field, there is a fairly good mixing of elements.

X-ray diffraction analysis of ceramics samples was performed using a Rigaku Miniflex 600 X-ray diffractometer. It can be used for qualitative and quantitative phase analysis of polycrystalline materials as well.

The research results were presented in the form of ordinary spectrograms with high resolution. Table 2 shows the results of X-ray analysis in the form of a table with processed spectra. The table 2 also presents for comparison the results of X-ray diffraction analysis of phosphors of the SDL series and yttrium oxide powder. The space group of all phosphors and ceramics samples is Ia-3d and of yttrium oxide - Ia-3. The lattice parameters are represented in the table 1.

Table 2. X-ray analysis of prepared ceramics samples

Composition of sample	Type of phase	lattice parameters, Å	Note
YAG:Ce Al ₂ O ₃ (59.5 %) + Y ₂ O ₃ (23.8 %) +Gd ₂ O ₃ (11.9%)+Ce ₂ O ₃ (4.8 %)	YGd ₃ Al ₅ O ₁₂ :Ce	a= 12.064519 b= 12.064519 c= 12.064519	20 peaks corresponds to phases YGd ₃ Al ₅ O ₁₂ :Ce
YAG:Ce	Y ₃ Al ₅ O ₁₂ :Ce	a= 12.012482 b= 12.012482	20 peaks corresponds to phases Y ₃ Al ₅ O ₁₂ : Ce

Al_2O_3 (59.5 %) + Y_2O_3 (35.7 %) + Ce_2O_3 (4.8 %)		$c = 12.012482$	
Y_2O_3 – pure	Y_2O_3	$a = 10.615582$ $b = 10.615582$ $c = 10.615582$	32 peaks corresponds to phases Y_2O_3
SDL 2700	$\text{YGd}_3\text{Al}_5\text{O}_{12}:\text{Ce}$	$a = 12.074755$ $b = 12.074755$ $c = 12.074755$	31 peaks corresponds to phases $\text{YGd}_3\text{Al}_5\text{O}_{12}:\text{Ce}$
SDL 3500	$\text{Y}_3\text{Al}_5\text{O}_{12}:\text{Ce}$	$a = 12.022043$ $b = 12.022043$ $c = 12.022043$	20 peaks corresponds to phases $\text{Y}_3\text{Al}_5\text{O}_{12}:\text{Ce}$
SDL 4000	$\text{Y}_3\text{Al}_5\text{O}_{12}:\text{Ce}$	$a = 12.009555$ $b = 12.009555$ $c = 12.009555$	36 peaks corresponds to phases $\text{Y}_3\text{Al}_5\text{O}_{12}:\text{Ce}$

Thus, in the synthesized ceramics samples the main phase is YAG phase, just like in YAG phosphors.

4. Luminescence and excitation spectra of YAG ceramics

Luminescence spectra of samples and excitations spectra of the luminescence were measured with a CM 2203 spectrophotometer. Figure 4 shows the luminescence spectra of the synthesized ceramics samples excited by light with a wavelength of 345 nm. The luminescence spectra are characteristic of YAG:Ce and YAGG:Ce phosphors [6-8]. In the latter, some yttrium ions are replaced by gadolinium ions. It leads to shift of luminescence band to red region (figure 4). Luminescence spectra of ceramics samples of the same composition are similar.

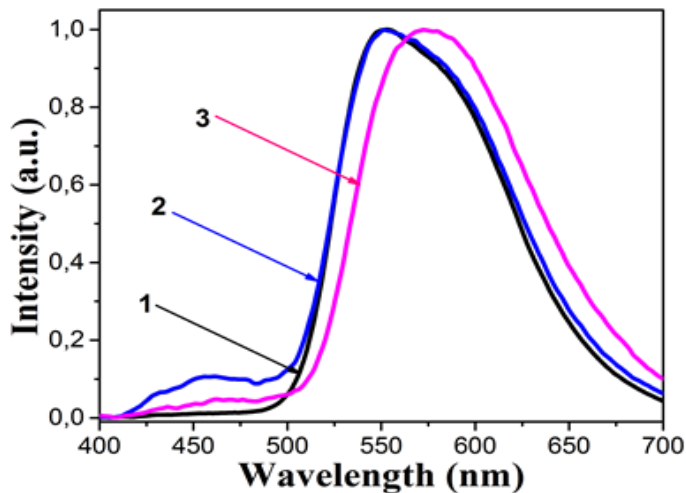


Figure 4. Luminescence spectra of ceramics samples of the different composition: (1, 2) - Al_2O_3 (59.5 %) + Y_2O_3 (35.7 %) + Ce_2O_3 (4.8 %); (3) - Al_2O_3 (62 %) + Y_2O_3 (25 %) + Gd_2O_3 (13 %) + Ce_2O_3 (1 %).

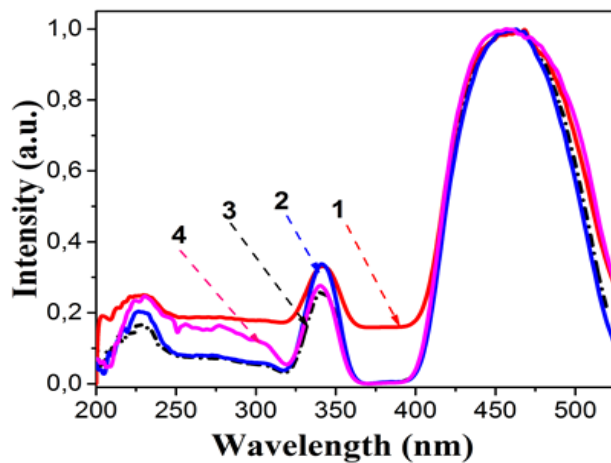


Figure 5. The excitation spectra of the emission in the ceramics samples of the different composition: (1) - Al₂O₃ (59.5 %) + Y₂O₃ (35.7 %) + Ce₂O₃ (4.8 %); (2) - Al₂O₃ (56.8 %) + Y₂O₃ (34.1 %) + Ce₂O₃ (9.1 %); (3) - Al₂O₃ (56.8 %) + Y₂O₃ (34.1 %) + Ce₂O₃ (9.1 %); (4) - Al₂O₃ (56.8 %) + Y₂O₃ (22.7 %) + Gd₂O₃ (11.4 %) + Ce₂O₃ (9.1 %).

Figure 5 shows excitation spectra of the luminescence at the maxima of the bands in the ceramics samples with different elemental composition. Three bands in the excitation spectra at 450, 340 and 220 nm in YAG:Ce phosphors are observed.

5. Discussion

The results of studies showed that ceramic based on yttrium-aluminum garnet, doped with cerium and synthesized in the radiation field, luminescence quite well when excited by radiation in a wide UV spectral range. The spectral characteristics of luminescence and excitation are quite similar to those measured for YAG:Ce phosphors. In the prepared ceramics the main phase is YAG: Ce (or YAGG: Ce) phase. Although the morphology of ceramics is very different from microcrystals of YAG: Ce phosphors, the luminescence characteristics indicate that nanodefects responsible for luminescence [9, 10] are formed in crystallites. Obviously, further standard processing of ceramics to transform it into a phosphor: crushing and annealing at temperatures of 1500–1700 K, will make it possible to obtain significantly better quantitative characteristics of the luminescence.

It is known that ionizing radiation fluxes are used in practice, for example, to modify material properties. In [11], it was shown that dielectric samples are destroyed when exposed to powerful short pulses of electron flow. In [12], the possibility of ceramics sintering under exposure to powerful fluxes of low-energy electrons, about 15 keV, is shown. Using a powerful flow of electrons with such low electron energies (penetration depth of 10 nm) that leads only to heating and emission. The mean of the free path of electronic excitations is about 10 nm as well. Therefore, to melt the refractory oxides, the flow of electrons can be directed not to the charge, but to the graphite crucible in which the charge is placed.

It is known to use powerful stream of high-energy electrons for effects on materials properties (1.4 MeV, penetration depth of electrons is about 2.5 mm). The layer of metal powder melted under the electron flow on a metal surface [13]. But in the metal all the energy of the electron flow is converted into heat. The flow of electrons is used to the direct energy transfer to target. In [14] ceramics based on magnesium fluoride doped with tungsten was first successfully synthesized using a powerful flux of electrons with energy of 1.4 MeV. The synthesis of dielectric materials in the field of a high-power flux of high-energy electrons is fundamentally different from the synthesis in thermal fields. With the used irradiation modes, which make up 20 % of the maximum possibility of the accelerator, the bulk density of the absorbed energy during the exposure to the flow for 1 s is $8 \cdot 10^{23}$ eV/cm³.

During the synthesis in radiation field $\sim 12 \cdot 10^{22}$ electronic excitations (ionization, electron-hole pairs) are created in 1 cm³ of charge consisted of the oxide materials with an average band gap. The formation of structural phases occurs from a set of charge elements with a high degree of ionization, that is, with

dangling bonds. Therefore, it is possible to form structural phases from various combinations of atoms and ions participating in the process. Since Y_2O_3 , Al_2O_3 , Gd_2O_3 , Ce_2O_3 are dominant in the charge, the formation of the crystalline phase of YAG or YAGG with activator ions, cerium, distributed in it is most likely. During synthesis in thermal fields, only the core (atomic, ionic) subsystem is excited. The electronic subsystem remains unexcited. Unambiguous proof of the dominant role of ionization in the process of ceramics synthesis in the radiation field is the following. For the production of ceramics based on MgF_2 , the stream with a power of 18 kW was optimal, whereas for the synthesis of YAG: Ce ceramics - 22 kW. The melting point of MgF_2 is 1260 K, whereas the melting points of the components for the synthesis of YAG:Ce ceramics are in range from 2060 K (Al_2O_3) to 2450 K (Y_2O_3). For the synthesis of ceramics from components, the melting points of which differ by almost 2 times, flows of similar power are needed.

Note that during the synthesis in a powerful radiation flux, a significantly higher efficiency of the mixing of charge components is achieved. This is evident from the results of the study of the spatial distribution of elements in ceramics. It should be expected that the obtained composition of ceramics will be closer to the initial one in the charge than during the synthesis by other methods.

References

- [1] Ye S, Xiao F, Pan Q, Ma Z and Zhang Q 2010 *Materials Science and Engineering reports* **71** 1–34
- [2] Pan Y, Wu M and Su Q 2004 *Materials Science and Engineering B* **106** 251–56
- [3] Silveira L G D., Cótica L F., Santos I A., Belançon M P, Rohling J H and Baesso M L 2012 *Materials Letters*. **89** 86–89
- [4] Fadlalla M H, Tang CC, Wei S Y. and Ding X X. 2008 *J. Lumin.* **128** 1655–59
- [5] Yang H.J. [et al.] 2012 *J. Am. Ceram. Soc.* **95** 49–51
- [6] Liu Z, Liu S, Wang K and Luo X 2010 *Applied Optics* **49** 247–57
- [7] Lisitsyn V M., Soshchin N P, Yu Yang yang, Stepanov S A, Lisitsyna L A, Tulegenova A T, and Abdullin Kh A. 2017 *Russian Physics Journal* **60** 862–65
- [8] Lisitsyn V M, Abdullin Kh A, Stepanov S A, Tulegenova A T 2016 *Izv.Vuzov.Physics* **59** 164–68
- [9] Lisitsyna L A, Oleshko V I., Putintseva S N. and Lisitsyn V M 2008 *Optics and Spectroscopy* **105** 531–37
- [10] Lisitsyna L A, Lisitsyn V M 2013 *Physics of the Solid State* **55** 2297–2303
- [11] Dolgachev G I, Kazakov E D, Kalinin Yu G, Malinin S A, Maslenikov D D and Sadovnichii D N 2018 14th International Conference on Modification of Materials with Particle Beam and Plasma Flow *EFRE* 2018 238
- [12] Dvilis E S, Burdovitsyn V A, Khasanov A O, Oks E M, Klimov A S, Zenin A A, Khasanov O L 2016 *Fundamentalnie issledovania* **10** 270–79
- [13] Golkovski M G, Samoylenko V V., Polakov I A, Bataev V A and Chakin I 2018 3rd International Conference on New Materials and Haigh Technologies, *EFRE* 2018 622.
- [14] Lisitsyn V M, Lisitsyna L A, Dauletbekova A, Golkovskii M, Karipbayev Zh T, Musakhanov D, Akilbekov A, Zdorovets M, Kozlovskiy A and Polisadova E 2018 *Nuclear Inst. and Methods in Physics Research B* **435** 263–67